Unraveling the spectroscopy of coupled intramolecular tunneling modes: A study of double proton transfer in the formic-acetic acid complex

Michael C. D. Tayler,[a] Bin Ouyang,[b] and Brian J. Howard[c]
Physical and Theoretical Chemistry Laboratory, South Parks Road, Oxford OX1 3QZ, United Kingdom

(Received 27 October 2010; accepted 26 November 2010; published online XX XX XXXX)

The rotational spectrum of the *hetero* dimer comprising doubly hydrogen-bonded formic acid and acetic acid has been recorded between 4 and 18 GHz using a pulsed-nozzle Fourier transform microwave spectrometer. Each rigid-molecule rotational transition is split into four as a result of two concurrently ongoing tunneling motions, one being proton transfer between the two acid molecules, and the other the torsion/rotation of the methyl group within the acetyl part. We present a full assignment of the spectrum $J = 1$ to $J = 6$ for the ground vibronic states. The transitions are fitted to within a few kilohertz of the observed frequencies using a molecule-fixed effective rotational Hamiltonian for the separate A and E vibrational species of the G_{12} permutation-inversion symmetry group. Interpretation of the motion problem uses an internal-vibration and overall-rotation angular momentum coupling scheme and full sets of rotational and centrifugal distortion constants are determined. The tunneling frequencies of the proton-transfer motion are measured for the ground A and E methyl rotation states as 250.4442(12) and −136.1673(30) MHz, respectively. The slight deviation of the latter tunneling frequency from being one half of the former, as simple theory otherwise predicts, is due to different degrees of mixing in wavefunctions between the ground and excited states. © *2011 American Institute of Physics*. [doi:10.1063/1.3528688]

I. INTRODUCTION

Hydrogen bonding sits in a central position in the investigation of noncovalent intermolecular interactions. Among complexes thus formed, carboxylic acid dimers again occupy an important position. This can be attributed to (1) the favorable process of dimerization, even at room temperature, due to the particularly strong hydrogen bonds formed, and (2) the ubiquitous occurrence of the carboxylic group and analogs of double-proton transfer in organic, atmospheric, and biological chemistry.

To study the detailed nature of these systems, gas-phase spectroscopic methods are widely used. The most stable geometries of dimers formed between trifluoroacetic acid and formic, acetic and monofluoroacetic acids were found this way by the pioneering microwave spectroscopic study in 1964 by Costain and Srivastava.[1] In these cases the pair of carboxyl groups binds cooperatively as both a proton donor and acceptor, forming a large eight-membered ring containing two hydrogen bonds. Improved spectral resolutions and structures were obtained after a revisit by Bauder and co-workers in 1990 using a jet expansion.[2] Extensive studies by Bellott and Wilson on dimers between trifluroacetic acid and many other carboxylic acids indicated further that the feature of eight-membered ring exists in virtually all carboxylic acid dimers in the gas phase.[3]

While only *hetero* dimers can be studied by microwave spectroscopy, other high-resolution methods such as femtosecond degenerate four-wave mixing and Raman spectroscopy can be applied to complexes without permanent electric dipole moments, notably formic[4] and acetic acid[5] *homo*-dimers. Assignments of the inter- and intramolecular vibrational modes of the formic acid dimer in its centrosymmetric, lowest energy geometry were recently used to probe both the harmonic and anharmonic parts of the potential energy surface.[6,7]

Aside from structure, these techniques may be used to retrieve information on the nuclear dynamics, in particular the concerted double proton transfer motion between the two parting acid molecules. Vibrational splittings may arise in the spectra as the direct manifestation of this tunneling motion, and with analysis estimates of the proton transfer energy barriers and the hydrogen bond strengths can be made. Again in $(HCOOH)_2$ Havenith and co-workers successfully observed the tunneling phenomenon, and reported upon this in extensive works.[8–11] Splittings of 0.0158(4) cm^{-1} for the ground state and 0.0100(3) cm^{-1} for the first excited C=O stretch state[9] were seen in the most abundant isotopic species. Theoretical investigations showed attempts at reproducing the measured tunneling frequencies, interpreting the actual reaction path, and unraveling the coupling of the proton transfer motion with the normal vibrational modes for the dimer. Other carboxylic acid dimers, e.g., benzoic and substituted benzoic acid dimers are found to exhibit similarly fast tunneling motions, both in vapor and in the condensed phase.[12–14]

Herein, we report the spectroscopy of the formic-acetic acid *hetero* dimer, $HCOOH–CH_3COOH$ (FA–AA). Despite intensive studies on its class, this simple molecule has

[a]Present address: School of Chemistry, Southampton University, SO17 1BJ, UK.
[b]Present address: Department of Chemistry, University of Cambridge, Lensfield Road, Cambridge CB2 1EW, UK.
[c]Electronic mail: brian.howard@chem.ox.ac.uk.

always been seen missing in the spectroscopic investigation of acid dimer complexes. This should not be due to any experimental difficulty since both acids have high enough vapor pressures at room temperature for a gas phase spectrum to be easily recorded. Neither that the two acids have "missed" each other accidentally because they are the two simplest carboxylic acids and are normally used in these studies as "starting" molecules within their homologs. They have indeed been included in the same study for a few times in the past.[1,2,15] As shown in this paper, the likely reason is that the two concurrent tunneling motions present in this seemingly simple dimer—these being the double-proton transfer previously observed in the formic acid dimer, and in addition the torsion of the methyl group in acetic acid—severely complicate the assignment and fitting of its spectrum.

The FA–AA dimer is not an isolated example of two simultaneously ongoing tunneling motions. An almost identical molecule, theoretically speaking, is methylmalonaldehyde (MMA) whose rotational spectrum was first recorded and analyzed by Sanders.[16] Intramolecular transfer of the enol proton plus the torsion of the methyl group produce a *four-fold* vibrational splitting in the spectrum. Chou and Hougen,[17] and Ilyushin *et al.*,[18] report the spectrum of MMA at higher resolution with reanalysis of the degenerate E torsional states using an improved theory to attempt a better description of the internal angular momentum.

Two other very similar systems 5-methyltropolone and 5-methyl-9-hydroxyphenalenone were studied by Nishi *et al.* using fluorescence and hole-burning spectroscopy.[19,20] Proton transfer between the C=O and enol C–OH groups plus the torsion/internal rotation of a rather remote methyl group were again found to couple with each other. The methyltropolone has since been subject to theoretical investigations aimed at correlating these nuclear dynamics with *ab initio* electronic energy surfaces.[21]

Besides the above, many other molecules undergo two tunneling motions at the same time including methylamine[22–24] and *p*-cresol,[25] both studied at rotational resolution and both possessing the same permutation-inversion symmetry as FA–AA.[26] In these cases, inversions of protons between two mirror images of the same molecule are observed, rather than the proton transfer motion noted above which must involve chemical bond cleavage and reformation.

In one of the more successful high-resolution analyses, reasonable values of the internal rotation parameters for methylamine were determined using Ohashi and Hougen's phenomenological Hamiltonian.[22,23] The residual of the least-squares fit, though, was much larger than the experimental accuracy. For *p*-cresol internal rotation parameters were also determined, yet, the tunneling frequency of the proton inversion was mainly extracted by fitting spectrum of the A internal rotation state only.[25]

We will show here that the rotational spectrum of FA–AA can be fitted using a new Hamiltonian approach, a major improvement over Hougen's phenomenological one being that all parameters in this case have ready physical interpretations. The solution involves consideration of various vibration-rotation coupling terms and treatment of these terms

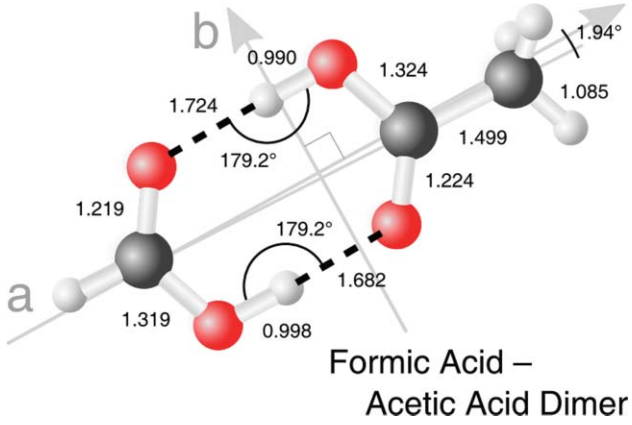

FIG. 1. Geometry of FA–AA determined via MP2 6–311++G (2df, 2pd) with selected bond lengths (in Å), angles and the a, b principal axes indicated. The 1.94° refers to the angle made between the principal a and the C–C bond axes.

using multiple levels of perturbation theory. It will be shown the perturbation effects sometimes generate terms that can be merged with others if they happen to contain the same operator, thus resulting in the mixing of different fitting parameters. Removal of this mixing effect is necessary if "clean" rather than convolved parameters are desired. Indeed, molecular structural information such as the relative orientations of the principal axis system, the proton-tunneling-averaged axis system, and the methyl rotor can only be properly determined after this treatment.

As an example relevant to both the topics of carboxylic acid dimers and multidimensional tunneling this study of FA–AA emphasizes: (i) obtaining accurate structural information; namely, the principal moments of inertia and the methyl bond axis orientation, for what is considered in spectroscopic terms a "large" nonrigid molecule; (ii) the kHz-accurate determination of a tunneling frequency for the intriguing double proton transfer between the two acid monomers, providing again another strong experimental benchmark for theoretical calculations on these coupled vibrations.

II. STRUCTURE OF THE FA–AA COMPLEX

Figure 1 shows a geometry for FA–AA optimized using the GAUSSIAN 03 package.[27] Initially a calculation was made at the level of MP2 6–31+G (2df, 2pd), then refined using a more extensive 6–311++G (2df, 2pd) basis plus counterpoise correction to minimize basis-set superposition error. A near-prolate asymmetric rotor, the global minimum-energy conformation yields the principal rigid-rotor constants $A = 5.816$ GHz, $B = 1.336$ GHz, $C = 1.094$ GHz. The rather dissimilar lengths of the hydrogen bonds, 1.724 and 1.682 Å, are almost identical to those calculated for the formic acid-propriolic acid mixed dimer.[28] The list of all atom coordinates is available in the electronic supporting material.[29]

Principal components $\mu_a = 0.9$ D and $\mu_b = 0.1$ D of the dipole moment were estimated from the MP2 charge density. The small magnitude of μ_b confirms Fourier-transform microwave spectroscopy more suitable for recording the b-type transitions of this complex than microwave absorption

spectroscopy as the intensities depend only linearly on the magnitude of transition dipole, not quadratically as for the latter method.

An indication of accuracy in the calculated structure is the planar moment of inertia $P_c = (I_{aa} + I_{bb} - I_{cc})/2$, which should be zero for a truly planar molecule. It is convenient, here, to picture FA–AA as a slightly asymmetric planar "frame" (incorporating the two carboxylic groups) to which the methyl rotor is attached. As the molecule overall retains C_s point symmetry, two methyl hydrogens are the only atoms lying outside the ab inertial plane resulting in a small $P_c = 1.58$ uÅ.^{2} This figure confirms all heavy atoms like C and O are essentially confined to the ab plane, neglecting zero-point motion.

III. SPECTROSCOPIC THEORY

A. Molecular symmetry formulation

The scheme in Fig. 1 indicates six isoenergetic conformational minima are accessible through operations involving torsion of the methyl and double hydrogen transfer between the two acid molecules. Viewed from the frame of the dimer these rearrangements may be seen to occupy a two-dimensional potential, $V(z, \phi)$, (Fig. 2) in which the collective motions of the nuclei involved are factored onto two independent vibrational degrees of freedom. A periodic coordinate, ϕ, encapsulates the torsion of the methyl group corresponding to movement within the threefold-symmetric potential about the C–C bond. The set of operations, namely (123), (132) and $\hat{e}$ of the C_3 permutation-inversion (PI) symmetry group[26] generates the A and E torsion/internal rotation states of the methyl group while leaving the other part of the complex intact. The spatial part of the total nuclear wavefunction, ψ, transforms in this representation as

$$(123)\psi(z,\phi) \equiv \hat{a}\psi(z,\phi) = \psi(z,\phi + 2\pi/3); \qquad \hat{a}^3 = \hat{e}. \tag{1}$$

The double proton transfer motion plus an accompanying 60° torsion of the CH_3 group may be expressed by the symmetry operation $\hat{b} = (23)(45)^*$, (for brevity the swapping of C and O labels are omitted, since these nuclei are bosons. The labels 4 and 5 denote the protons membered inside the hydrogen bonds, as also seen in Fig. 2). The second coordinate, z, then accounts for the geometric repositioning of atoms around the ring where the two monomers are bound. The sign change of z reminds us of the reversal in the direction of the b-principal inertial axis during the proton transfer:

$$\hat{b}\psi(z,\phi) = \psi(-z,\phi + \pi/3); \qquad \hat{b}\hat{b} = \hat{a}. \tag{2}$$

The simultaneous double proton transfer and methyl rotation in FA–AA is termed "inversion" for it is *isomorphic* to the amine inversion in methylamine. Yet similarities do not stop here. The operations $\hat{a}$ and $\hat{b}$ are the generators of the molecular permutation-inversion group G_{12}, this being the same PI symmetry group describing the pattern of intramolecular motion in the methylamine also, and unsurprisingly, this is true also of all the previously mentioned systems involving coupled methyl torsion plus one other large-amplitude vibration (see Sec. I and also Refs. 22 and 26 for extensive reviews). It is well-known that the inversion motion in each case splits the A and E vibronic states further into + and − symmetric levels across the proton tunneling. The following secular model envisages these six lowest-energy vibronic states as linear combinations of the localized, noninteracting, ground states "χ_i" for each minimum $i = 1, 2, \ldots, 6$ in the two-dimensional potential:

$$\begin{aligned} &\chi_1,\ \chi_2,\ \chi_3,\ \chi_4,\ \chi_5,\ \chi_6, \\ \psi^{A-[4\times1]} &= (+1,+1,+1,-1,-1,-1)/\sqrt{6}, \\ \psi^{E+[6\times2]} &= (+2,-1,-1,+2,-1,-1)/\sqrt{12} \\ &\quad (0,+1,-1,\ \ 0,+1,-1)/2, \\ \psi^{E-[2\times2]} &= (+2,-1,-1,-2,+1,+1)/\sqrt{12} \\ &\quad (0,+1,-1,\ \ 0,-1,+1)/2, \\ \psi^{A+[12\times1]} &= (+1,+1,+1,+1,+1,+1)/\sqrt{6}, \end{aligned} \tag{3}$$

where the χ's are numbered as in Fig. 2. In square brackets the superscripts give the associated Fermi statistical weights predicted after reducing also the spin wavefunction, in the G_{12} representation. We shall refer to the energy separations between the ± levels as the "tunneling splittings," ν_{-+}, which are related in this model to the $\hat{b}$-type tunneling matrix

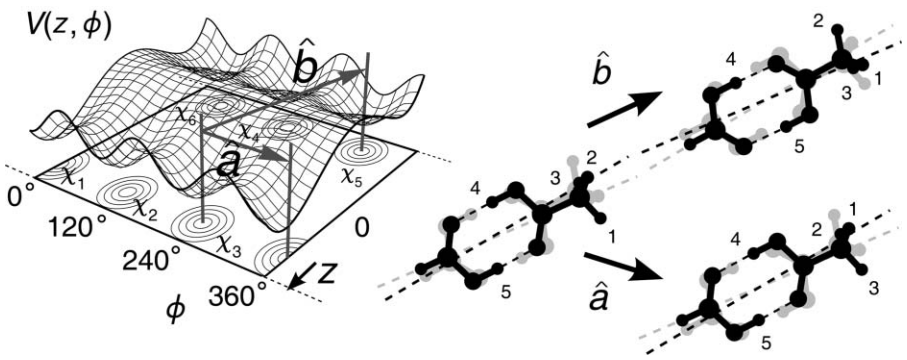

FIG. 2. Representation of two-dimensional tunneling and G_{12} permutation-inversion symmetry operations of the formic-acetic acid dimer. If the geometrical readjustments are assumed to proceed in a smooth and concerted manner, trajectories $\hat{a}$ and $\hat{b}$ are both symmetric degenerate rearrangements and the hindering two-dimensional potential $V(z, \phi)$ has point symmetry D_{3d}.

elements:

$$\nu_{A-+} = \varepsilon_{A-} - \varepsilon_{A+} = -4\langle\chi_i\,|\hat{V}(z,\phi)\,\hat{b}\,|\,\chi_i\rangle,$$
$$\nu_{E-+} = \varepsilon_{E-} - \varepsilon_{E+} = +2\langle\chi_i\,|\hat{V}(z,\phi)\,\hat{b}\,|\,\chi_i\rangle. \quad (4)$$

The ratio −2, evident from this simple theory, will be questioned during a more quantitative modeling of the two-dimensional tunneling in due course.

B. Hamiltonian

Complications arise in the spectral analysis due to the existence of the two tunneling motions. Firstly each rotational level is split into four, from the four distinct tunneling symmetry species. Also the expectation value of the internal angular momentum, $\boldsymbol{\xi}$, is nonzero and therefore couples to the end-over-end rotational angular momentum $\boldsymbol{P}$ of the complex to contribute to the total *quantized* angular momentum $\boldsymbol{J}$ of the system. This coupling can displace the transition frequencies from those of a rigid rotor, perhaps by as much as > 1 GHz.

Occurrences of $\boldsymbol{P}$ in the rotational Hamiltonian are therefore replaced by

$$P_a^2 = (J_a - \xi_a)^2,\ P_b^2 = \ldots. \quad (5)$$

This substitution has appeared many times before to address the spin-orbit coupling (L-doubling) phenomenon in diatomic molecules and also in the vibration-rotation spectra of high-symmetry molecules such as CH_4.[30] It is assumed Coriolis contributions from the regular low-amplitude normal modes are small and can be neglected. For a molecule of low point-symmetry possessing no degenerate vibrational normal modes, this approximation is very good to a first order level of estimation. In the principal axis system (PAS) the full rotational and large-amplitude vibrational Hamiltonian can therefore be expressed by the following:

$$H^{P} = A^{P}(J_a - \xi_a)^2 + B^{P}(J_b - \xi_b)^2 + C^{P}(J_c - \xi_c)^2 + \hat{T}_{int} + V(z,\,\phi) + H_{cd}^{P}. \quad (6)$$

The terms on the top line approximate the pure rotational kinetic energy of the molecule where A^{P}, B^{P}, and C^{P} are the principal rotational constants assuming the methyl group (whose rotation gives part of the internal angular momentum $\boldsymbol{\xi}$) in the molecule is structureless. In other words, when the three hydrogen atoms in this group are taken to lie on their collective centre of mass rather than extending out like an umbrella. The whole complex with this "structureless" methyl group is quoted as the frame, here and afterwards. Definition of the rotational constants this way is necessary because the rotational kinetic energy of the methyl protons is already implied in the $\hat{T}_{int}$ operator for the total internal kinetic energy on the line below. The conventional Watson-reduced centrifugal distortion Hamiltonian, H_{cd},[31] absorbs the angular momentum terms from the couplings with the "normal" low-amplitude vibrational levels.

Equation (6) is a correct formulation of the dynamics problem but it is not the most convenient form available. As for any molecule possessing the G_{12} PI symmetry, the contributions to $\boldsymbol{\xi}$ from each of the z and ϕ coordinate motions are seen to lie at right angles. In FA–AA, these would be: (i) in the ab inertial plane, the pure methyl torsion angular momentum, which is to be regarded by the operator $\hat{j} = -i\hbar\partial/\partial\phi$; (ii) the angular momentum about the c-axis generated during the "pure" (z-only) double proton transfer rearrangement. The latter may be eliminated by shifting to the nonprincipal axis system of the "average" PAS at $z = 0$; this is abbreviated as the "AAS." While there is a price of an off-diagonal inertial term F_{ab} associated with the operator $(P_a P_b + P_b P_a)$ in the rotational constants matrix coming from this transformation, the resulting AAS Hamiltonian is advantageous because it contains now only angular momentum operators for the rotating methyl group and the whole molecular rotation overall (the superscript ^{A} denotes the AAS):

$$H^{A} = A^{A}(J_a - \lambda_a j)^2 + B^{A}(J_b - \lambda_b j)^2 + C^{A}J_c{}^2 + F_{ab}^{A}[(J_a - \lambda_a j)(J_b - \lambda_b j) + (J_b - \lambda_b j)(J_a - \lambda_a j)] + \hat{T}_{int} + V(z,\,\phi) + H_{cd}^{A}. \quad (7)$$

This has been written in terms of the direction cosines λ_a and λ_b made between the C–C bond and the AAS a and b axes, given that $\xi_a = j\lambda_a, \ldots,$ etc., in the AAS. Note that $\lambda_c = 0$, since $\langle j\rangle$ is perpendicular to the c axis.

From this point, the Hamiltonian is translated into a set of fitting parameters to the energies of the rigid-rotor basis ($|JK_aK_c\rangle$) for each of the tunneling symmetries. Similar to the Born–Oppenheimer approximation in separating the electronic-vibrational motion, one may separate the $+-/AE$ tunneling problem from the rotational one. First, as they are unconnected by the Hamiltonian (7), the A/E pairs can be treated as different molecules with the expectation value of the angular momentum, i.e., with $\langle j\rangle$ of the A state strictly zero, yet the E state nonzero. Each $\pm$ pair then needs only to be characterized by the tunneling separation, as determined by the two-dimensional problem $\hat{T}_{int} + V$ [see Eq. (4)].

The new operators in Eq. (7) involving terms such as $J_\alpha j$ are to be tackled using perturbation theory, seeing that they do not have eigenfunctions $|JK_aK_c\rangle$ in general because they can mix both the vibration and rotational states (see Sec. III C). The corrections at first order are simply the coefficients of J_α, so evidently perturb just the E states:

$$D_a J_a = -2(A^{A}\lambda_a + F_{ab}^{A}\lambda_b)\,\langle j\rangle\,J_a, \quad (8)$$

$$G_b\,J_b = -2(B^{A}\lambda_b + F_{ab}^{A}\lambda_a)\,\langle j\rangle\,J_b. \quad (9)$$

Different symbols are used here, i.e., D and G, to emphasize that the first one acts only between rotational states of the same vibrational symmetry while the second connects those which are opposite. The matrix elements of $D_a J_a$ between the $+$ and $-$ states are zero because $2(A^{A}\lambda_a + F_{ab}^{A}\lambda_b)$ transforms symmetrically during the $\hat{b}$ tunneling motion, so only the $\pm \leftrightarrow \pm$ ones can remain finite. For the analogous J_b term the vanishing elements should be the other way around. This follows because λ_b and F_{ab}^{A} change sign during the proton transfer, making the operator antisymmetric across this motion.

Coriolis terms also yield second order corrections that are quadratic in J_a and J_b, through the mixing of excited tunneling states. These behave as though they are modifying the

proper rotational constants to give so-called "effective" constants, which are the ones to be fitted from the spectrum:

$$A^{\text{eff}} = A^{\text{A}} - 4\left(A^{\text{A}}\lambda_a + F_{ab}^{\text{A}}\lambda_b\right)^2\Sigma, \tag{10}$$

$$B^{\text{eff}} = B^{\text{A}} - 4\left(B^{\text{A}}\lambda_b + F_{ab}^{\text{A}}\lambda_a\right)^2\Sigma, \tag{11}$$

$$F_{ab}^{\text{eff}} = F_{ab}^{\text{A}} - 4\left(B^{\text{A}}\lambda_b + F_{ab}^{\text{A}}\lambda_a\right)\left(A^{\text{A}}\lambda_a + F_{ab}^{\text{A}}\lambda_b\right)\Sigma'. \tag{12}$$

The strength of these deviations is proportional to the sum

$$\Sigma' = \sum_{m\neq 0} \frac{\langle \pm 0|\, j \,|\mp m\rangle\,\langle \mp m|\, j \,|\pm 0\rangle}{\varepsilon_m - \varepsilon_0}, \tag{13}$$

that connects the ground ($m = 0$) to each mth excited methyl torsion state across the $\pm \leftrightarrow \mp$ symmetries. (Σ is identical here, but connecting $\pm \leftrightarrow \pm$). So unlike the first-order ones, the second order effects are nonvanishing for both the A and E states.

Finally, the terms in j^2 act as corrections to the rotational constant of the methyl group. This can be best understood as the *effective* methyl rotational constant since during the torsion motion, the rest of the molecule rotates to the opposite direction which will effectively reduce its moment of inertia. Because J_α is not involved here, differences in $\boldsymbol{j}$ between the +/− states can expect to show as distortions to the ν_{-+} splittings.

C. Microwave selection rules

The allowed rotational transitions in FA–AA must possess nonzero values of the transition dipole for at least one projection of the electric dipole moment operator.

To start with, as there is no term in the Hamiltonian capable of connecting the A and E torsion states, rotational transitions may only occur as $A \leftrightarrow A$ and $E \leftrightarrow E$. The a- and b-type transitions, those induced by the μ_a and μ_b components of the dipole moment, then obey vibration selection rules according to their transformation under the G_{12} group. The internal part of μ_a is symmetric for the proton exchange motion, so it has nonzero matrix elements within the + and − states and all a-type transitions should occur as $+ \leftrightarrow +$ or $- \leftrightarrow -$. The internal part of μ_b on the other hand changes sign under the proton transfer operation and is only capable of inducing transitions between the + and − inversion states.

For the rotational part of the wavefunction also the selection rule is more complicated than a normal asymmetric top molecule with no internal angular momentum. This is due to the terms linear in J_a and J_b in the effective Hamiltonian of the E torsional state after we expand Eq. (7) [see also, e.g., Eq. (10) in Ref. 32]. The matrix elements of the term $G_b J_b$ in the standard $|J K_a K_c\rangle$ prolate top basis set is small (cf. $\lambda_b \ll 1$) in regard to the spacing between the levels it is connecting and for this reason its mixing effect is usually small in the spectrum. The term linear $D_a J_a$, however, is capable of connecting the two K_a doublets with the same J and in many cases its matrix element is comparable to or even *greater than* the asymmetric doubling spacing. The resulting in-mixing between the two K_a doublets activates the following normally forbidden transitions:

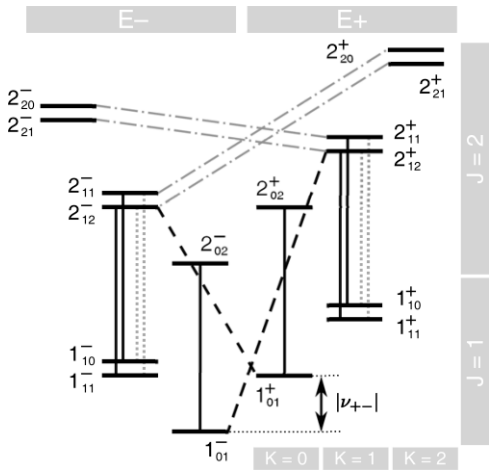

FIG. 3. Scheme of allowed microwave transitions for FA–AA. The *solid lines* and *thick dashes* show conventional a- and b-dipole transitions. The methyl internal rotation mixes the K-doubling levels by the $D_a J_a$ term (see text), allowing the otherwise-forbidden a-dipole transitions (*dots*) plus a nominally forbidden Q-branch (*dots and dashes*).

$$a\text{-dipole:} \quad \Delta K_a = 0, \Delta K_c = 0, 2, \Delta J = 1, \tag{14}$$

$$b\text{-dipole:} \quad \Delta K_a = 1, \Delta K_c = 1, \quad \Delta J = 0, 1. \tag{15}$$

The transitions $2^{\pm}_{1,0} \leftarrow 1^{\pm}_{1,0}$ for instance will now possess a certain finite intensity due to this mixing effect, strong enough to detect with our instrument. Figure 3 illustrates these additional transitions; they make available the exact energy pattern up to $K_a = 2$ for the E states.

IV. EXPERIMENTAL

The microwave spectrum was recorded between 4 and 18 GHz using a pulsed-nozzle Fourier transform spectrometer based on the design of Balle and Flygare.[33,34] Details of this apparatus are given in previous work.[35]

Microwave pulses of length 1.0 μs were introduced via an L-shaped antenna into a Fabry–Perot cavity comprising two near-confocal aluminum mirrors each with radius of curvature 50 cm. The separation of the mirrors is adjustable by stepper motor in the vicinity of 60 cm, to tune the cavity toTEM_{00} resonant modes for greatest radiation density along the beam axis, with a natural bandwidth of 0.5–1.0 MHz at the desired frequency. A vacuum of $< 10^{-4}$ mbar is held in the chamber by an oil diffusion pump.

Formic and acetic acids were available at reagent grade and used without further purification. Helium at a pressure of 3 atm was bubbled through a 3:17 volume mixture of HCOOH: CH_3COOH at room temperature, forming a reservoir of *homo* and *hetero* acid dimers in the gas phase. This corresponds to a 1:1 mol vapor in the rare-gas carrier. The sample was introduced to the cavity via a 0.5 mm diameter pulsed nozzle mounted within the fixed mirror, with the jet undergoing supersonic expansion. Translational temperatures below 2 K are obtained as the combined result of adiabatic cooling and narrow divergence of the molecular beam.

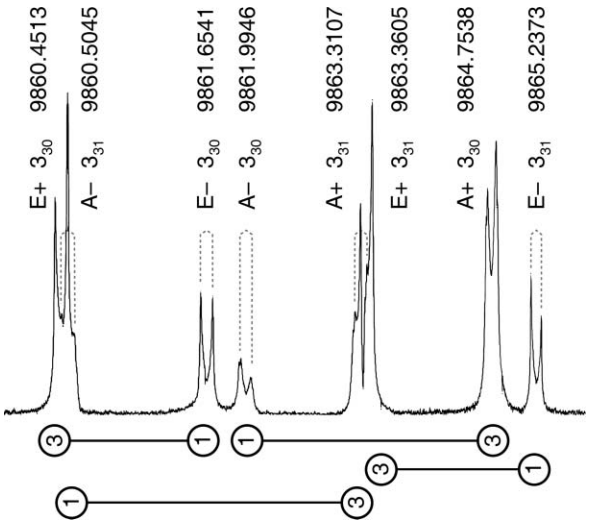

FIG. 4. Crowding of a-type rotational transitions starting from $J_{K_a} = 3_3$ in the region 9860–9866 MHz. For these quantum numbers the nuclear spin statistics decide transitions starting from the "+"/"−" vibrational levels occur with weights 3:1, as indicated below the baseline.

The microwave emission is detected through the antenna as a free-induction decay (FID), mixed down onto a carrier of frequency 2.5 MHz and then digitized by means of a 10 MHz A/D card before further analysis is carried out on a personal computer. The data acquisition and recording procedure is fully automated, permitting FIDs to be sampled at a rate of typically 14 Hz.

V. SPECTRAL ASSIGNMENT AND ANALYSIS

The A E and $\pm$ doubling together with the activation of the nominally forbidden transitions causes the FA–AA spectrum to become highly complicated compared to the "rigid" molecule as there are over four times as many rotational lines. In total we measured 74 Doppler doublets up to and including those from $K_a = 5$ sublevels of the A tunneling states, plus a further 110 for the E species. These collectively amount to the full set of allowed a- and b-type transitions accessible over the entire spectrometer operating range (4–18 GHz).

Despite the relative crowding of transitions the lines can be unambiguously fitted as there are many clues to their identities. For instance all of the transitions in the A subspectra broadly match the AAS rotational energy patterns for a rigid FA–AA geometry because the correction terms in Eqs. (8)–(12) amount merely to small changes in the rotational and centrifugal distortion constants. In the case of the $E \leftrightarrow E$ transitions the a-type lines with $|K| = 1$ are readily identified as these are the ones most strongly perturbed by the D_a coupling, having separations of gigahertz between the $K_a K_c$ doublets. As noted earlier, the A and E sets can be fitted independently, giving an extended check of self-consistency. The nuclear-spin intensity weighting property of Eq. (3) is also invaluable to making the correct assignment when many transitions are closely spaced, e.g., in the higher ($K_a \geq 3$) asymmetric doublets, as Fig. 4 shows.

To fit Eq. (7) and the effective parameters in Eqs. (8)–(12), we used our own purpose-made least-squares program based upon the Levenberg–Marquardt iteration, similar to Pickett's SPFIT.[36] Up to 20 *completely general* fitting parameters may be accommodated in this program by specifying each respective operator in matrix form. Each iteration involves the assignment of rotational quantum numbers to the energy eigenvalues of each K_a block of the Hamiltonian matrix representation, for each of the four tunneling symmetries. The corresponding eigenvectors are used to find the derivatives of the transition frequencies with respect to the fitting parameters. From these, updated parameters for the next cycle of the convergence can then be calculated.

Table I shows the result of the fits. An assignment of the A state a-type transitions based from the *ab initio* rotational constants was possible using an eight-parameter model comprising $A^{\text{eff}}(\pm)$, $B^{\text{eff}}(\pm)$, $C^{\text{A}}(\pm)$, F_{ab}^{eff} and the tunneling splitting $\nu_{A-+} = \varepsilon_{A-} - \varepsilon_{A+}$. The sensitivity to the tunneling parameter lies in the second-order effect of F_{ab}. This fitting gave $\nu_{A-+} = 250 \pm 5$ MHz on the a-type transitions alone, and enabled a reasonable prediction of the b-type transitions frequencies. Then after including the b-type transitions, originating from states with $K = 0$, (that due to the small size of μ_b, could only be excited on increasing the microwave power by a factor of 10), and after introducing the centrifugal distortion terms the fitting yielded $\nu_{A-+} = 250.44$ MHz and gave a root-mean-square of 0.28 kHz in the obs-calc frequency differences. This is a very good fit, given the measurement uncertainty of each line is about ± 1 kHz.

The $E \leftrightarrow E$ transitions were fitted via a similar "progressive refinement" to a 15-parameter model now including the energy level perturbations arising at odd perturbation orders in $J_\alpha j$ (1st, 3rd, ...). These are also listed in Table I.

One of the interesting values to determine is $\langle j \rangle$, which is calculable from the fitted parameters using equation 8 or 9. The ratio $D_a(-)/D_a(+)$ shows that $\langle j \rangle$ of the *lower-energy* $E-$ state is in fact higher than that of the $E+$ state, by 0.63%. Though this difference is marginal, it may arise due to differences in the vibrational wavefunctions. Unlike its symmetric counterpart, the function ψ^{E-} goes zero at $z = 0$, as of symmetry, meaning it may have delocalized further into the classically forbidden region between minima connected by the pure methyl torsion. This extra penetration would result in a larger internal angular momentum of the antisymmetric symmetry species as implied by the fitting constants.

The other linear term, $G_b J_b$, has nonzero matrix elements connecting the $E+/E$-states and was therefore fitted as a "shared" parameter between these two states. We did not pin down a precise value for G_b until the inclusion of the μ_b-allowed R- and Q-branch transitions, or in other words, until the exact $E\pm$ energy level positions were known. With only the a-type data the fit was poor and very insensitive to G_b, for it could otherwise easily be mimicked by combined shifts in the energies from the tunneling splitting ν_{E-+} and first-order effect of F_{ab}. The current fit, with the cross-tunneling transitions included, allows a concerted and unambiguous determination of the F_{ab}^{eff}, G_b, and ν_{E-+} terms together. While the tunneling frequency $\nu_{E-+} = -136.17$ MHz is only approximately minus-half that of the A states, not exactly as

TABLE I. Effective parameters from the least-squares fits of rotational transitions in the formic acid- acetic acid dimer.[29]

Parameter	Operator	$A+$	$A-$	$E+$	$E-$	Unit
$(A-\overline{B})^{\text{eff}}$	J_a^2	4646.4036(15)	4646.2370(39)	4561.3614(62)	4561.5037(61)	MHz
$\overline{B}^{\text{eff}}$	J^2	1233.6136(10)	1233.6063(12)	1233.4745(8)	1233.4825(8)	MHz
$(B-C)^{\text{eff}}/4$	$J_+^2 - J_-^2$	63.3387(59)	63.3380(52)	63.2824(3)	63.2803(3)	MHz
D_a	J_a	–	–	1418.9759(28)	1427.3503(31)	MHz
F_{ab}^{eff}	$J_aJ_b + J_bJ_a$	170.66(29)		167.110(19)		MHz
G_b	J_b	–		34.511(70)		MHz
Δ_a	J_a^3	–		−1.5771(4)		MHz
ν_{-+}		250.4442(12)		−136.1673(30)		MHz
D_J	$-(J^2)^2$	0.2047(38)		0.20351(5)		kHz
D_{JK}	$-J^2J_a^2$	1.2766(220)		1.2578(200)		kHz
D_K	$-J_a^4$	0.0224(39)		−10.3(7)		kHz
d_1	$J^2(J_+^2 - J_-^2)$	−0.0398(43)		–		kHz
d_2	$J_+^4 - J_-^4$	−0.006 18(260)		–		kHz
Number of transitions		74		110		
rms fit		0.28		6.74		kHz

predicted by the secular model in Eq. (4), one must consider that shifts due to perturbation corrections can contribute, *viz.* $(A^{\text{A}}\lambda_a^2 + B^{\text{A}}\lambda_b^2)(\langle j^2(+)\rangle - \langle j^2(-)\rangle)$ from the methyl kinetic energy. There can always be some in-mixing from higher torsion-vibrational states too. This again proves the torsion of the methyl group and the transfer of the protons are coupled together.

Resolvable effects on the rotational energy levels were also detected for the high-order terms, including: a cubic term in J_a, or $\Delta_a J_a^3$ as shown in Table I comes from the third-order effect of $-2A^{\text{A}}jJ_a$ after the expansion of Eq. (7), in similarity to hydrates of acetic acid previously studied in our group.[32] The value of Δ_a from spectrum fitting agrees very well with that obtained by solving the methyl torsional problem and is hence physically reasonable. Its effect is however a factor 10^2 less than D_aJ_a and practically identical for both inversion symmetries. The analogous, yet-smaller, fourth-order term is absorbed into the D_K parameter of the Watson Hamiltonian for the centrifugal distortion (as they are associated with the same operators) and again justifies a "shared" effective H_{cd} for both proton transfer symmetries. This rapid decay in successive perturbation orders confirms FA–AA lies in the so-called *high-barrier* rotation limit, where the methyl torsion is strongly hindered.

Higher than quadratic order in λ_b, terms such as the third-order J_b^3 correction are omitted, since $\lambda_b^3 \approx 0$. Overall this fitting of the E spectrum is very satisfactory with the root-mean-square deviation in the residual (observed minus calculated) frequencies being 6.7 kHz, which is unprecedented for a G_{12} molecule interpreted directly inside a molecular-frame Hamiltonian formalism.

VI. RECOVERY OF SPECTROSCOPIC PARAMETERS

As mentioned earlier, the spectrum fitting parameters (shown in Table I) contain contributions from multiple spectroscopic constants due to the torsion-rotation coupling. Some analysis is required to obtain the "proper" constants before informative dynamics and structural details about the complex can be derived.

In principle, only the first and second-order Eqs. (8)–(12) are needed to fit deterministically the unknowns $\langle j(E+)\rangle$, $\langle j(E-)\rangle$, λ_b, A^{A}, B^{A}, and $\Sigma(A\pm/E\pm)$ to the values of the effective constants given in Table I. A more meaningful approach, however, is to tackle the original Hamiltonian [Eq. (6)] directly, assuming appropriate mathematical forms for the potential $V(z,\phi)$ and the kinetic energy T_{int}. Solving the wavefunctions and the vibronic energies will give the *exact* tunneling splittings, *exact* internal angular momenta and the corrections to the rotational constants. This route has the benefit of determining the energy barriers to the proton transfer and methyl torsion motions. To demand a physically more convincing fit of all the information available so far, the higher perturbations, e.g., Δ_a, can also be included in this process.

A simple potential with all the correct symmetry properties is as follows:

$$V(z,\ \phi) = V_3(1-\cos 3\phi)(z/2z_0) + V_2(1-z^2/z_0^2)^2 \qquad (16)$$

with minima occurring at $V(z_0,\ 0) = 0$, $V(-z_0,\ \pi/3) = 0\ldots$, etc., and a barrier of V_2 at $z/z_0 = 0$ when the three-fold term goes to zero. Therefore, V_2 and V_3 represent the respective energy barriers to motion along z and ϕ between the minima. The torsion one, V_3, is especially interesting as there are many examples from similar CH_3CO groups and conjugated molecules to compare, both spectroscopic and calculated.[32,37] Our *ab-initio* calculations show the trajectory of the total electronic potential $V(z_0,\ 0\rightarrow\pi/3)$ [determined by counterpoise corrected MP2 6–311++G(2df,2pd)] fits to a single cosine function $V'(\phi) = V_3'(1-\cos 3\phi)/2$ with V_3' = 137.1 cm^{-1} which is a reasonable estimate although zero-point vibrational effects are ignored.

The internal kinetic energy term, in the same dimensionless coordinates,

$$T_{\text{int}} = Fj^2 - b\ \partial^2/\partial(z/z_0)^2, \tag{17}$$

may be more difficult because some knowledge is needed about F and b, which are related to the masses undergoing motion. The coefficient F equates to a rotational constant of the methyl group about the C–C bond. This is however easily enough approximated in the PAS by the rotational constant of methane (spherical rotor, $F_{\text{Me}} = 5.24\ \text{cm}^{-1}$). In the AAS,

$$F = F_{\text{Me}} + A^{\text{A}}\lambda_a^2 + B^{\text{A}}\lambda_b^2 + F_{ab}^{\text{A}}\lambda_a\lambda_b, \tag{18}$$

where the last three terms denote the correction to the rotational constant of the methyl group by the molecular frame; basically the frame rotates along a reversed direction to the methyl group during the torsional motion, and this results in a decrease in the effective torsional moment of inertia and increase in the effective rotational constant. The other part of Eq. (17), briefly, involves a constant b which is similar to a c-type inertia constant in the sense that all tunneling atoms move in the ab plane during the proton transfer motion, and their movements generate an angular momentum along the c axis. Working in the AAS, b must correspond to the inverse of a moment of inertia written as $\Sigma_i m_i z_{0i}^2$ where z_{0i} is half the distance traveled by each atom (of mass m_i) across the proton transfer.

The simulations were performed by setting up the matrix representation of $\hat{T}_{\text{int}} + \hat{V}$ in a sufficiently large harmonic-oscillator / free-rotor product basis to obtain, on diagonalization, convergent values for the vibrational energies and the perturbation coefficients up to third order in J_a. A two-step iteration procedure was then applied: (i) starting from estimates of V_2 and V_3, b, F, the values of $\langle j(E\pm)\rangle$, Σ, ν_{+-} were calculated; (ii) with these calculated values and with the fitted parameters in Table I, Eqs. (8)–(12) were solved to obtain the constants A^{A}, B^{A}, F_{ab}^{A}, λ_a and λ_b. (N.B. while $\lambda_a^2 \equiv 1 - \lambda_b^2$ we must still determine the relative sign). This method must be "self-consistent" because steps (i) and (ii) each on their own do not make the problem deterministic. Instead, step (ii) depends upon the kinetic and potential terms in (i) being accurate. One iteration therefore proceeds, for instance, by modifying values of the V_2 and V_3 barriers and inspecting the quality of the fit after step (ii), then judging updated barriers. This continues until the "best" fit in the final spectroscopic constants is reached, meaning we obtain: (a) a common set of pure rotational constants A^{A}, B^{A}, F_{ab}^{A} from each vibrational symmetry state; (b) both tunneling splittings in agreement with the experiment. These finally decontaminated values of A^{A} and B^{A} plus the best-fit parameters of the internal Hamiltonian are listed in Table II.

As $V_2 \gg V_3$ would indicate, the ratio V_3/F is strongly correlated with j. Hence, because $\langle j(E)\rangle$ is determined very accurately from the spectrum fitting, the value of V_3 can also be known very precisely, given F is also well determined. This figure $V_3 = 107.0\ \text{cm}^{-1}$ is consistent with what is regarded as a "high" methyl torsion barrier where one finds a small magnitude of the methyl angular momentum. Compare in the free-rotor limit $V_3 = 0$ that $\langle j\rangle$ should be 1 for the ground E state. The value obtained here is $|\langle j(E)\rangle| \approx 0.12$.

TABLE II. Determination of the pure spectroscopic constants which are self-consistent with the barriers fitted to the potential $V(z,\phi)$. N.B. $\theta = \arctan(\lambda_b/\lambda_a)$. The inertia coefficients F and b were not optimized in these fits.

		$A+$	$A-$	$E+$	$E-$
A^{A}	MHz	6046.488	6046.490	6046.939	6046.951
B^{A}	MHz	1360.392	1360.382	1360.226	1360.229
$\lvert j\rvert$		…	…	0.1174	0.1181
F_{ab}^{A}	MHz	174.751		173.745	
ν_{-+}	MHz	243.14		−129.01	
λ_b	…	−0.0193	$V_3\ \text{cm}^{-1}$	107.0 ± 0.1	
λ_a	…	+0.9998	$V_2\ \text{cm}^{-1}$	8000 ± 100	
θ^{A}	degrees	−1.12	$b\ \text{cm}^{-1}$	68.6	
			$F\ \text{cm}^{-1}$	5.25	

The V_3 barrier implies, nevertheless, that the CH_3 group in FA–AA is considerably less hindered than in monomeric acetic acid, (where $V_3 \approx 165\ \text{cm}^{-1}$).[38] It is rather similar to the acid dimers like CF_3COOH:$HOOCCH_3$ ($V_3 \approx 97.1\ \text{cm}^{-1}$), supporting the hypothesis of a much more symmetrical electron distribution around the adjacently bonded carbon.[2]

V_2 was most sensitive to the tunneling frequencies and the differences between the + and − rotational constants. The extremely large value of $V_2 \approx 8000\ \text{cm}^{-1}$ is in line with the inversion barriers estimated in Ref. 1 for CF_3COOH-$HCOOH$ (greater than $6000\ \text{cm}^{-1}$) and CF_3COOH-CH_3COOH (less than $5000\ \text{cm}^{-1}$) arguing that stronger hydrogen bonds may indicate an increased electron density between the two acid monomers. This must be taken with caution, though, because we have no direct access to the value b. The estimate of $68.6\ \text{cm}^{-1}$ used in these fits was calculated on the outcome of our *ab initio* structure and the guessed transformation route between the initial and final two proton transfer states. Further accuracy in b demands a more careful analysis of the structural changes during the proton transfer motion, e.g., by making an isotopic substitution study. However, despite the approximations we have made, the barriers should not possess large errors.

It is also possible to derive the relative orientations of the AAS and PAS frames and the direction of the methyl rotor axis within them. With the values for the pure A^{A}, B^{A} and F_{ab}^{A} terms, we calculate the angle between the a axes of the AAS and PAS to be 2.1°. One can compare this with the same quantity predicted using the *ab initio* optimized structure. By averaging the two equivalent minimum structures of FA–AA before and after the proton transfer, with coordinates expressed in the PAS, we obtain an *approximation* to the effective (AAS) axis system. Recall the AAS is the one in which the c- internal angular momentum associated with the proton transfer motion is zero. In order to satisfy the Eckart conditions[39] of zero angular action, an angle of 2.1° is required, which is identical to that obtained above. This quite remarkable self-consistency is partly due to cancelation of errors; however, it also validates the convincingly fitted barriers of the effective potential, the reliability in the *ab-initio* structure, and the theoretical interpretation of the rotational spectrum.

Finally, the direction cosines λ_a and λ_b supply an angle $\theta^{\mathrm{A}} = \arctan(\lambda_b/\lambda_a) \approx -1.1^\circ$ between the AAS a-axis and the methyl rotor. Combining this angle with the one above, relating the PAS to the AAS, we would expect to deduce the methyl orientation within the PAS, (θ^{P}). While it may appear that there is a choice of taking the sum or difference of these angles there is in fact only one combination correct with the Eckart formulation of the effective axes system. This is deduced because the sign of the inertial constant F_{ab}^{A} is well-defined according to the sense of the c-axis rotation used to transform between the two reference frames. The Eckart condition fixes the direction of the a and b inertial axes in each frame, depending on the sign of this rotation. As the direction of the methyl angular momentum is already known in the AAS, from the signs of G_b and D_a, it follows that the relative signs of F_{ab}^{A}, G_b and D_a should pin down the three angles without ambiguity. Our analysis indicates, for the signs used, the methyl rotation axis lies $\theta^{\mathrm{P}} = (-1.1^\circ - 2.1^\circ) = -3.2^\circ$ from the principal a-axis, where the sign is correct with the axes convention in Fig. 1.

The value -3.2° for θ^{P} may not be in perfect agreement with the *ab-initio* result of -1.94°, yet the geometrical difference can be reasonably accounted within the errors of the calculation. It should be noted we have observed similar deviations between the calculated and spectroscopically determined geometries of the weakly bound acetic acid hydrate complexes.[32]

VII. SUMMARY

Spectroscopic analysis of FA–AA provides an excellent opportunity to examine theory in a molecule with simultaneously ongoing tunneling motions. The major challenge is to produce a self-consistent assignment of the congested rotational spectrum, for which to date only a limited range of comparable molecules have been studied. A transparent and simple interpretation of the internal-vibrational angular momentum shows to be highly successful for unraveling the tunneling dynamics and determining interesting details about both the dynamics *and* structure of the complex.

We hope the present method's simplicity renews the inspiration to study, at high resolution, similarly large and "loose" molecules where there is more than one large-amplitude internal motion present. Here FA–AA provides insight into the influence of a neighboring CH_3 group upon intermolecular hydrogen-bonding. It is also the first structural study of the molecule published in the literature, filling a long-standing gap in the homologous study of carboxylic acid dimers.

Only the normal CH_3/H_2 isotopic species is studied in this analysis. In future the CD_3/H_2 and CH_3/D_2 isotopologs may also be considered to make a more extensive review of the internal potential surface, as well as to properly quantify the effective masses moving along each internal tunneling coordinate z and ϕ.

ACKNOWLEDGMENTS

The work was part-funded by the EPSRC–UK. The author M.C.D.T. wishes to thank Corpus Christi College, Cambridge for generous financial support. B.O. expresses thanks to the Chinese Ministry of Education and University of Oxford for jointly providing the China/UK scholarship for excellency to support his study in the UK.

[1] C. Costain and G. Srivastava, J. Chem. Phys. **41**, 1620 (1964).
[2] L. Martinache, W. Kresa, M. Wegener, U. Vonmont, and A. Bauder, Chem. Phys. **148**, 129 (1990).
[3] E. M. Bellott and E. B. Wilson, Tetrahedron **31**, 2896 (1975).
[4] V. V. Matylitsky, C. Riehn, M. F. Gelin, and B. Brutschy, J. Chem. Phys. **119**, 10553 (2003).
[5] C. Riehn, V. V. Matylitsky, M. F. Gelin, and B. Brutschy, Mol. Phys. **103**, 1615 (2005).
[6] R. Georges, M. Freytes, D. Hurtmans, I. Kleiner, J. V. Auwera, and M. Herman, Chem. Phys. **305**, 187 (2004).
[7] Z. Xue and M. A. Suhm, J. Chem. Phys. **131**, (2009).
[8] F. Madeja and M. Havenith, J. Chem. Phys. **117**, 7162 (2002).
[9] M. Ortlieb and M. Havenith, J. Phys. Chem. A **111**, **7** 355 (2007).
[10] A. Gutberlet, G. W. Schwaab, and M. Havenith, Chem. Phys. **343**, 158 (2008).
[11] O. Birer and M. Havenith, Ann. Rev. Phys. Chem. **60**, 263 (2009).
[12] C. S. Tautermann, M. J. Loferer, A. F. Voegele, and K. R. Liedl, J. Chem. Phys. **120**, 11650 (2004).
[13] C. K. Nandi, M. K. Hazra, and T. Chakraborty, J. Chem. Phys. **121**, 7562 (2004).
[14] C. K. Nandi, M. K. Hazra, and T. Chakraborty, J. Chem. Phys. **123** (2005).
[15] E. M. S. Macoas, P. Myllyperkio, H. Kunttu, and M. Pettersson, J. Phys. Chem. A **113**, 7227 (2009).
[16] N. D. Sanders, J. Mol. Spectrosc. **86**, 27 (1981).
[17] Y. C. Chou and J. T. Hougen, J. Chem. Phys. **124**, 074319 (2006).
[18] V. V. Ilyushin, E. A. Alekseev, Y. C. Chou, Y. C. Hsu, J. T. Hougen, F. J. Lovas, and L. B. Picraux, J. Mol. Spectrosc. **251**, 56 (2008).
[19] K. Nishi, H. Sekiya, H. Kawakami, A. Mori, and Y. Nishimura, J. Chem. Phys. **111**, 3961 (1999).
[20] K. Nishi, H. Sekiya, T. Mochida, T. Sugawara, and Y. Nishimura, J. Chem. Phys. **112**, 5002 (2000).
[21] O. Vendrell, M. Moreno, and J. M. Lluch, J. Chem. Phys. **117**, 7525 (2002).
[22] N. Ohashi and J. T. Hougen, J. Mol. Spectrosc. **121**, 474 (1987).
[23] N. Ohashi, S. Tsunekawa, K. Takagi, and J. T. Hougen, J. Mol. Spectrosc. **137**, 33 (1989).
[24] V. Ilyushin and F. J. Lovas, J. Phys. Chem. Ref. Data **36**, 1141 (2007).
[25] A. Hellweg and C. Hattig, J. Chem. Phys. **127**, (2007).
[26] P. R. Bunker and P. Jensen, *Fundamentals of Molecular Symmetry* (Taylor & Francis, London, 2004).
[27] M. J. Frisch, G. W. Trucks, H. B. Schlegel *et al.*, GAUSSIAN 03, Revision C.02, Gaussian, Inc., Wallingford, CT, 2004.
[28] A. M. Daly, P. R. Bunker, and S. G. Kukolich, J. Chem. Phys. **132**, 201101 (2010).
[29] See supplementary material at http://dx.doi.org/10.1063/1.3528688 for full list of assigned frequencies, list of atomic coordinates.
[30] M. Johnston and D. M. Dennison, Phys. Rev. **48**, 868 (1935).
[31] J. K. G. Watson, in *Vibrational Spectra and Structure*, edited by J. R. Durig (Elsevier, Amsterdam, 1977), Vol. 6, p. 1
[32] B. Ouyang and B. J. Howard, Phys. Chem. Chem. Phys. **11**, 366 (2009).
[33] T. J. Balle, E. J. Campbell, M. R. Keenan, and W. H. Flygare, J. Chem. Phys. **72**, 922 (1980).
[34] T. J. Balle and W. H. Flygare, Rev. Sci. Instrum. **52**, 33 (1981).
[35] R. J. Low, T. D. Varberg, J. P. Connelly, A. R. Auty, B. J. Howard, and J. M. Brown, J. Mol. Spectrosc. **161**, 499 (1993).
[36] H. M. Pickett, J. Mol. Spectrosc. **148**, 371 (1991).
[37] L. H. Spangler, Annu. Rev. Phys. Chem. **48**, 481 (1997).
[38] J. Demaison, A. Dubrelle, D. Boucher, J. Burie, and B. P. van Eijck, J. Mol. Spectrosc. **94**, 211 (1982).
[39] S. M. Ferigle and A. Weber, Am. J. Phys. **21**, 102 (1953).